

Addendum to
the SoLID Updated Preliminary Conceptual Design Report

The SoLID Collaboration

March 4, 2024

Contents

1	Executive Summary	1
2	Introduction and Update to Physics Case	2
3	Magnet Test	3
4	Pre-R&D Activities	4
4.1	Gas Cherenkov	4
4.1.1	High Luminosity Tests of Cherenkov with Electron Beam	4
4.1.2	HGC Tank and Magnetic Shielding	5
4.1.3	Mirror Blanks and Support	6
4.1.4	Mirror Coating	6
4.2	ECal and SPD	7
4.2.1	Design updates	7
4.2.2	ECal test at FTBF 2021	8
4.2.3	Detector test in JLab Hall C 2022-2023	8
4.3	GEM	9
4.4	Data Acquisition	11
5	Simulation and Software	12
6	Cost Estimation Update and Optional Cost Sharing Plan	14
	Bibliography	17
A	PAC 50 Report on SoLID-related Proposals	19

1 Executive Summary

This addendum is intended to provide several updates to the SoLID preliminary Conceptual Design Report (pre-CDR). The SoLID pre-CDR was initially presented by the collaboration to JLab in 2014 and was further refined three times. The most recent version, dated at the end of 2019 [1], was submitted to the DOE Office of Science, Nuclear Physics in 2020 as part of the SoLID MIE proposal. The purpose of this report is three-fold:

1. Provide an update on the Science case of SoLID that includes new proposals and how SoLID was received by the 2023 NSAC Long Range Plan (LRP).
2. Provide an update on the progress of collaboration activities since the writing of the last pre-CDR, in particular, the verification of the pre-conceptual design as a result of the pre-R&D activities.
3. Present a new budget estimate that reflects recent procurement quotations, labor costs, and a possible cost sharing plan with part of the cost covered by re-allocating part of the JLab operation and capital funds.

SoLID is designed to be a large-acceptance spectrometer that can handle high luminosity and process data at high rates. It is particularly suitable for measurements that require high statistics in multi-dimensional bins. The original SoLID program, established over a decade ago, was re-affirmed by a review of the science case articulated by the highly-rated original experiments by the JLab PAC in the summer of 2022. It included new proposals and run group proposals that were continuously developed for SoLID. Most recently, the SoLID spectrometer was prominently featured in the 2023 Long Range Plan by the Nuclear Science Advisory Committee (NSAC): In Recommendation 4 of the LRP, SoLID is explicitly listed as a project that will provide an opportunity to advance discovery. These updates to the SoLID scientific case are detailed in Section 2.

A central part of SoLID is the CLEO magnet which was moved from Cornell to JLab and assembled in the test lab. The necessary cryogenic infrastructure has been established, and a successful cold test has been performed. We describe the progress on the magnet test in Section 3.

Considerable progress has been made on pre-R&D activities of SoLID sub-systems. In Section 4, we first describe updates and pre-R&D activities on the detector systems. For the Cherenkov and ECal, we have performed two beam tests of their prototypes in Hall C at JLab with high-luminosity, high-rates and high-background conditions similar to that of the proposed SoLID experiments. We used the proposed deadtime-less electronics that provides the waveforms of the signals instead of the timing and pulse-height distributions used for traditional DAQ systems. Many valuable lessons have been learned from these beam tests. In addition, we have performed detailed simulations of the test data to benchmark the SoLID simulations. Meanwhile, the ongoing JLab experimental program is helping answer some of the known challenges of SoLID. One such example is the performance of GEM tracking detectors under high luminosity. The ongoing SBS program is providing valuable lessons. We also describe updates on the design of the DAQ system and related pre-R&D activities at the end of Section 4.

General updates on Simulation and Software are provided in Section 5, followed by an updated cost estimation and a possible cost sharing plan in Section 6.

In summary, the SoLID science program remains compelling and continues to grow. It is well received and endorsed by the Nuclear Physics community, as reflected in the latest NSAC Long Range Planning process. Furthermore, no show-stopper has been identified in the SoLID conceptual design, and the technology required has been demonstrated continuously by our pre-R&D activities. At present, the SoLID program is shovel-ready, and a path forward to construct SoLID is being developed.

2 Introduction and Update to Physics Case

The SoLID science program was established in 2009-2012 with five primary experiments: Three proposed measurements of Transverse-Momentum-Dependent Parton Distributions (TMDs) via Semi-Inclusive Deep Inelastic Scattering (SIDIS) with polarized ^3He and proton targets [2–4]; a fourth proposed measurement aiming at understanding the origin of the proton mass and accessing the gluons gravitational form factors via measurements of near-threshold photo-production and electro-production of the J/ψ vector meson [5]; and a fifth proposed measurement to test the electroweak sector of the Standard Model at low energy and study hadronic physics in the high- x region [6] through Parity-Violating Deep Inelastic Scattering (PVDIS). In addition, a series of approved experiments will run simultaneously with the main experiments. These include Deep Exclusive Meson Production (DEMP) [7] and Time-like Compton Scattering (TCS) [8], which access the Generalized Parton Distributions (GPDs) and improve our knowledge of the spatial three-dimensional structure of the nucleon. In 2020, one more run group proposal [9] was approved to measure the transverse spin structure of the neutron g_2^n and its second moment d_2^n .

In July 2022, all five original SoLID proposals underwent a jeopardy review by the JLab Program Advisory Committee 50 (PAC50), and all were re-approved. Four of the five retain the highest rating (A). The fifth one was upgraded from A- to A. In addition, two new experiments were submitted to the same PAC and were approved, one to study the flavor dependence of the EMC effect using PVDIS with a ^{48}Ca target [10] and the other to study hadronic physics with two-photon exchange via a measurement of the beam-normal single-spin asymmetry (BNSSA) in DIS [11]. The relevant sections of the PAC50 report are given in Appendix A.

In 2023, a measurement of the Double Deeply Virtual Compton Scattering (DDVCS) process [12] was proposed. As opposed to the DVCS and TCS processes, which access GPDs along the line $x = \pm\xi$, DDVCS, where both the initial and final photons are virtual, is the only known process allowing one to investigate independently the (x, ξ) -dependence of GPDs, i.e., at $x \neq \xi$. The measurement requires a muon detector placed behind the magnet endcap and thus was submitted to PAC51 only as a letter of intent. More experimental proposals using SoLID are being developed, including the DIS and SIDIS measurements using a tensor-polarized deuterium target to explore the spin structure of the deuteron.

As seen from above, it is clear that the physics case of SoLID has only become more prominent in the past a few years and will continue to do so as its new capabilities of a large acceptance detector at the polarized luminosity frontier are discovered. SoLID remains a unique spectrometer designed to carry out high-precision measurements needed by frontier research in QCD and fundamental symmetry studies. In fact, in the 2023 Nuclear Science Advisory Committee (NSAC) Long Range Plan (LRP) “A New Era of Discovery” [13], most if not all of the physics topics to be measured with SoLID are featured: SoLID is cited multiple times in Section 3 “Quarks and Gluons, Understanding the Strong Nuclear Force”, owing to its impact on uncovering the three-dimensional structure of the nucleon (Fig. 3.4); In Sidebar 3.9 and Section 6.5, SoLID’s PVDIS program is showcased as a tool that will search for physics beyond the Standard Model, improve our knowledge of PDFs, and probing the EMC effect. SoLID is also highlighted in the Facilities section (Figs. 9.3 and 9.4). Lastly, in Recommendation 4 of the LRP, SoLID is explicitly listed as a project that will provide “*an opportunity to advance discovery.*”

In the meantime, several workshops were held, and more are being planned to promote collaboration and discussions between the theory and experimental community, such that the SoLID physics program will remain at the frontier of nuclear physics research presently and in the next decade. For the even longer term, there is the prospect of upgrading CEBAF to include a polarized positron beam [14, 15] and to increase its energy from 12 to 20+ GeV [16]. SoLID will still play a crucial role in widening the science landscape with both upgrades.

3 Magnet Test

The CLEO II's solenoidal magnet was chosen for SoLID. With a uniform axial central field of 1.5 T and a $\pm 0.2\%$ uniformity, a large inner space with a clear bore diameter of 2.9 m and a coil of 3.1 m diameter, the CLEO II magnet will provide a full azimuthal coverage and sufficient space to accommodate the detector components.

After the completion of all experimental runs at Cornell, the coils and cryostat of the CLEO II magnet were moved to JLab in 2016 and the return steel moved in 2019. A new Cryo Control Reservoir (CCR), that allows the CLEO II service turret to adapt to the JLab cryogenic system was designed and fabricated. A modern instrumentation and control system was also developed for testing.

The preparation work described above led to a successful low current cold test where preliminary data showed that the magnet is operational. Without the return iron installed, the test was limited to low currents to prevent stray magnetic fields from affecting nearby sensitive equipment in the test lab or spilling over to adjacent personnel space. On March 24th, 2023, the magnet was ramped up to a current of 120 A and was held for 30 minutes. The power supply output voltage was 1.15 V with a ramp-up rate of 0.5 A/s. No increase in coil voltages was observed during ramp-up or while at 120 A. Based on the flatline nature of the temperature curves during the test, the coil appeared to be superconducting. A 3-axis Hall probe was installed in the bore of the magnet during the test, and the recorded data matched well the TOSCA model simulation, see Fig. 1.

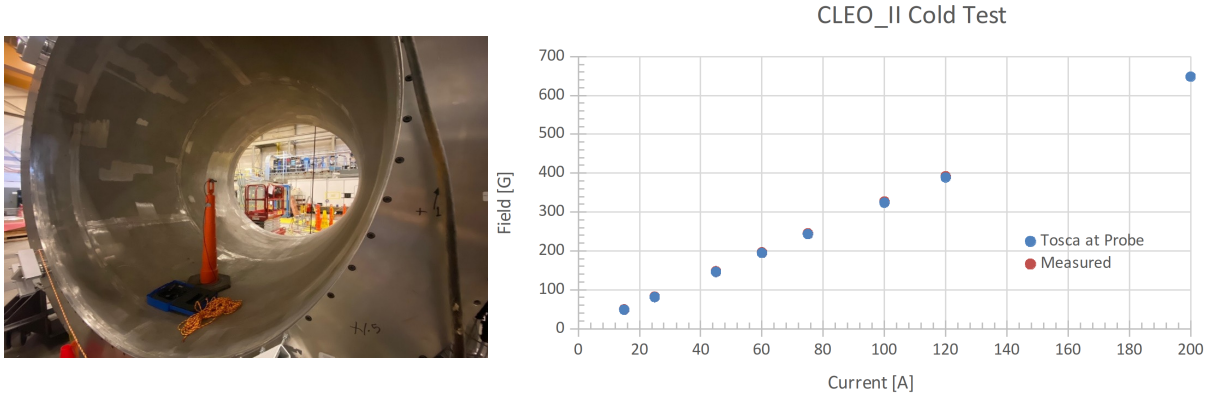


Figure 1: CLEO-II magnet cold test in March 2023. *Left:* A Hall probe was placed inside the magnet; *Right:* Measured field strength in Gauss (G) vs. current in Amp (A), compared to a TOSCA simulation showing good agreement. Note that the red dots are almost entirely covered by the blue dots. The test could only be done with low current due to safety regulations.

A standalone full-current test of the CLEO II magnet in the years leading up to the installation period of the SoLID experiment would provide several benefits. The first would be a fully functional test of the large solenoidal magnet with the return iron in a configuration capable of internally housing detectors for fixed-target experiments. The second would be to test the functionality of the cryogenic, instrumentation, and their control systems at the proposed experimental operating conditions. This would ensure the full functionality of the magnet for the SoLID experiments or any JLab experiments which may use this magnet.

To be ready for a full current test, JLab would need to provide the design/engineering labor and procurement cost for the long lead items associated with the modification of the existing CLEO II return iron as well as the new extended return iron associated with the detector housing.

4 Pre-R&D Activities

In the last several years, the SoLID collaboration has diligently carried out pre-R&D activities with the resources provided by the collaboration, JLab, and DOE/NP. The main goal of these pre-R&D activities was to optimize and validate the conceptual design and to reduce cost and schedule risks. Some of the pre-R&D activities, such as those related to data acquisition, greatly benefited the ongoing operation at the laboratory, examples are the SBS and NPS experimental programs. In turn, lessons learned from the SBS and NPS programs, which share the same expected high background, high rate, to some extent, with SoLID are invaluable to its program as well. We describe in this section the activities carried out on the Cherenkov (Section 4.1), ECal and SPD (Section 4.2), GEM (Section 4.3), and the DAQ system (Section 4.4).

4.1 Gas Cherenkov

SoLID has two Cherenkov detectors for particle identification, a light gas Cherenkov detector (LGC) for electron and charged pion separation and a heavy gas Cherenkov detector (HGC) for charged pion and kaon separation. The LGC will be used in both the PVDIS and the SIDIS- J/ψ configurations of SoLID while the HGC is used only in the latter. Both Cherenkov detectors need to operate in a high-rate and high-background environment. We report on two prototypes with two separate beam tests carried out under such conditions. There are also separate tests of the HGC pressured tank and its windows and a magnetic shielding required for the array of sixteen Multianode PMTs. A study of mirror blank fabrication and coating is also reported.

4.1.1 High Luminosity Tests of Cherenkov with Electron Beam

To better understand the impact of the expected high rate environment on the cherenkov detectors, two tests using two prototype detectors were performed in JLab's Hall-C using the electron beam.

The first test ran in 2018 and utilized a PVC telescopic tank with a sensor array of 2×2 Hamamatsu 64 pixel multi-anode PMTs (MaPMTs) coated with wavelength shifter (p-Terphenyl) capturing the Cherenkov radiation light reflected by a flat mirror at 90° . Two of the MaPMTs were from an older model H8500-03 and two were from the latest model H12700-03. During this period, a prototype LAPPD detector from INCOM was also tested. The Cherenkov detector was positioned at one fixed angle where electronics rates were estimated to peak around 1.5 MHz per PMT. The results of this test are summarized in Ref. [17].

A second Cherenkov prototype detector with a larger tank was built and tested in 2020 building on the successful initial prototype from 2018. This prototype, named the Telescopic Cherenkov Device (TCD), was able to accommodate an array of 4×4 Hamamatsu H12700-03 MaPMTs which matches the array size of the HGC design and is bigger than LGC's 3×3 design. The MaPMTs were all coated with a wavelength shifter (p-Terphenyl) to capture as much of the UV photons as possible. This test provided an opportunity to test additional electronic components including an analog summing board developed by the JLab detector group, a high-rate DAQ, and a newer model of INCOM's LAPPDs [18]. The TCD test ran parasitically in JLab's Hall-C and was positioned at two different locations in the hall to provide a low-rate (~ 320 kHz per PMT) and high-rate (~ 8 MHz per PMT) environment, comparing to the SoLID maximum rate of 4 MHz per PMT running condition. In both the low- and high-rate configurations, clean signals could be identified and overall electronics performance was nearly identical.

Both tests were successful in confirming our ability to measure and process high-rate signals and providing insight into better electronics configurations and analysis strategies. It was confirmed that using the Hamamatsu H12700-03 MaPMTs with the JLab designed summing electronics, that the devised

scheme of local coincidences between MAPMTs would suffice to mitigate any non-correlated random background hitting the sensors originating from the high luminosity environment. It was also determined that segmenting each MaPMT into summed quadrants would provide a better efficiency of determining signals. As a possible replacement for MaPMTs, large area picosecond photodetectors (LAPPDs) were also tested during the beam tests, with the results summarized in Ref.[18]. LAPPDs are known of being much more resilient to an external magnetic field compared to traditional PMTs. The prototype tests showed that the LAPPD supplied by INCOM for our test could operate as a replacement to the MaPMT array, but remain more costly than the MaPMT option with proper magnetic shielding. However, in synergy with INCOM's EIC HRPPD orders, the cost of an LAPPD or HRPPD may decrease to a level where it becomes on par with that of using the MaPMTs and their magnetic shielding.

The current plan moving forward is to use arrays of Hamamatsu H12700-03 MaPMTs with JLab designed summing electronics for both LGC and HGC detectors. We conclude that rates in excess of those expected could be handled without loss of efficiency of the sensors.

4.1.2 HGC Tank and Magnetic Shielding

The Heavy Gas Cherenkov detector (HGC) will use C_4F_8 gas at 1.7 atm absolute pressure to identify charged pions and suppress charged kaons over a momentum range of 2.5 to 7.5 GeV/c. Its tank will have a volume of about 20 m^3 and comprise 10 modules with a thin front window to reduce background. Shown in the left and middle of Fig. 2, a prototype tank of 1 module and a section of its neighboring module was designed at Duke University, then constructed and pressure tested at the University of Regina with Canadian funding support in 2021. It satisfies the engineering and safety requirements of JLab and was observed to have a low leak rate of $(9 \pm 2) \times 10^{-6}\text{ g/s}$ in 3-month long test.

The photosensor of each HGC sector covers an area of $20 \times 20\text{ cm}^2$. It needs to maintain good performance under the expected external magnetic field of $\sim 100\text{ Gauss}$ in the SoLID magnet endcap. We designed a magnetic shielding prototype made of 2 layers of low carbon iron and 1 optional inner layer of mu-metal, as shown in the right of Fig. 2. Our test showed that we can achieve a 20 G (5 G) field at the PMT location for a 90 G longitudinal (transverse) external magnetic field. This is good enough for the MAPMTs to operate with $<5\%$ gain loss. Our field simulation study further confirmed the test result.

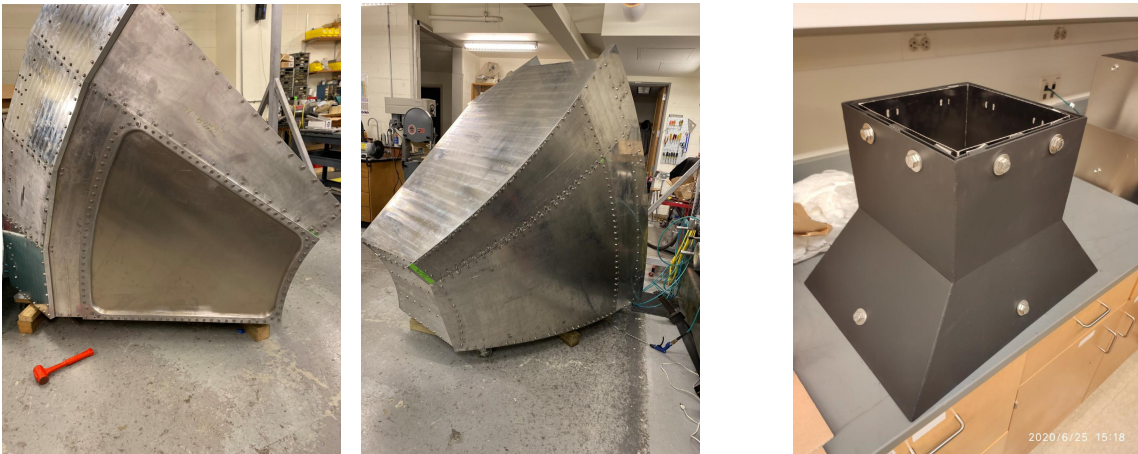


Figure 2: Left and middle: HGC tank prototype front and back view. Right: HGC magnetic shielding prototype.

4.1.3 Mirror Blanks and Support

To create mirrors that will least affect tracks passing through the Cherenkov detectors, a low-areal density solution for mirror materials is needed. Traditional glass mirrors typically have a trade-off in durability as the thickness of the mirror is reduced, creating practical issues with transport, handling and mounting. It is better to leverage carbon fiber reinforced polymer (CFRP) manufacturing to make sturdy and relatively thin blanks with none of the drawbacks of traditional glass. One disadvantage of CFRP blanks lies in the complexity in attaining a properly polished surface for UV reflection of Cherenkov radiation, but this can be overcome with innovative polishing techniques or the cost-effective inclusion of thin plastic layering that can be produced or polished much more easily.

The options for mirror blanks include:

- **Pre-fabricated CFRP:** The primary plan for Cherenkov mirror blanks for both the LGC and HGC is using cost-effective industrial manufacture of carbon-fiber-reinforced polymer spherical shell segments. The main question to explore is what minimum thickness of the shell can be achieved while maintaining the geometric design's tolerances.

Half-size proof-of-principle segments were ordered from Allred Inc, a designer and manufacturer of CFRP items for use in industry, aerospace, and defense to better test spherical shells. Early analyses of these segments show good rigidity and geometric consistency within millimeter tolerances. Allred Inc produced these segments at 1/16th of an inch thickness, giving the blanks an areal density of $< 3 \text{ g/cm}^2$, better than half the target areal density of 6 g/cm^2 . Tests are ongoing to confirm the accuracy of the radius of curvature, along with characterizing the expected deformation over time under normal stresses of mounting and operation.

- **3D printed CFRP:** Tests are also underway to determine the feasibility of 3D printed blank material as a cost-effective replacement for industrial-produced blanks. Beyond cost savings, 3D printed blanks allow for in-house production, finer detail over geometrical characteristics, and faster prototyping iteration. Significant challenges still remain, specifically in matching the uniformity, strength, and areal density.

Using industrial-produced CFRP blanks is currently the most reliable option, and it is the one we are pursuing for large scale production of the SoLID Cherenkov mirrors.

In addition to the blanks, a reflective surface that provides $> 85\%$ reflectivity into the UV is needed to achieve trigger efficiencies as quoted in the pre-conceptual design report. To best avoid the cost of a highly polished blanks, an intermediate plastic will be used as a base for the reflective coating. This type of mirror process has been pursued and effectively applied in the CLAS12 HTCC and LTCC Cherenkov detectors. The plastic film must have a small surface roughness (less than $1 \text{ }\mu\text{m}$) to achieve the desired UV reflection efficiencies. Companies like Evaporated Coatings Incorporated (ECI) can coat Lexan polycarbonate film to specifications for the LGC and HGC. Other plastics (PMMA acrylics or more exotic types such as Zeonex) can also achieve the required reflectivity. Aside from industrial coating, plastics may be directly coated by collaboration partners, which can provide the extra benefits of more control over the desired product. The Stony Brook University Nuclear Physics group has been testing coating plastic surfaces and is one such collaborator who could provide reflective coatings as described in the subsection below.

4.1.4 Mirror Coating

The Stony Brook Nuclear Physics group hosts an ultrahigh vacuum evaporation system that will be used to evaporate the manufactured mirror substrate surface (described in Sec. 4.1.3) with high optical quality in the target wavelength range from 180 to 600 nm. See Fig. 3.

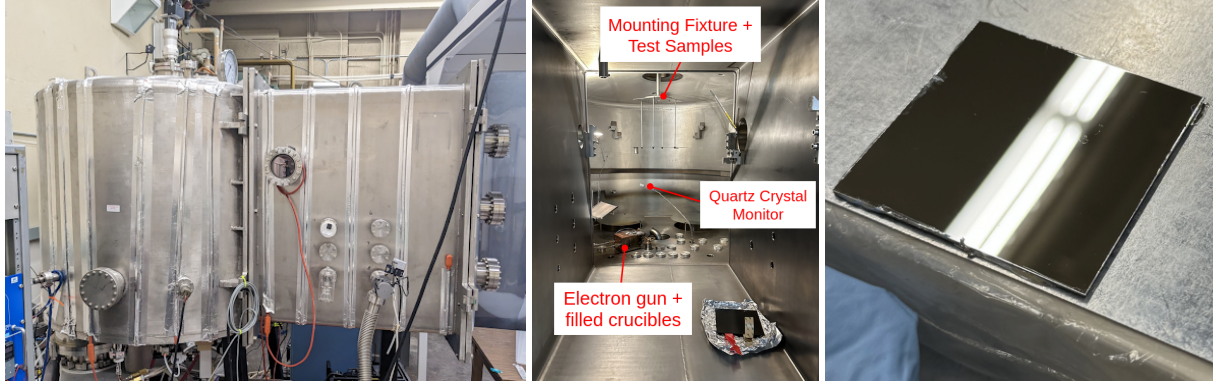


Figure 3: Left: side view of the evaporator at Stony Brook University Nuclear Physics group. Mid: evaporator interior and critical components. Right: Lexan-carbon fiber composite mirror sample coated at SBU.

The evaporation chamber consists of an integrated three-stage vacuum pumping system: roughing pump (10^{-3} Torr), turbo pump (10^{-6} Torr), and cryo pump (10^{-8} Torr). The substrates are mounted on a rotation stage rotating at 1 revolution/s to ensure the coated surface uniformity. The evaporator can accommodate mirror sizes as large as $80\text{ cm} \times 80\text{ cm}$. The strategy for coating the Cherenkov mirrors is to divide the long and narrow primary mirrors ($118.5\text{ cm} \times 43\text{ cm}$ in the x-y plane) into two segments; each segment will be coated separately to utilize the rotational mount to ensure coating uniformity.

The equipment configuration (shown in Fig. 3) can coat the substrate with a reflectivity of better than 75% at 300 nm, this capability was verified with a recent trial. The current coating vacuum quality is 3×10^{-6} Torr and will be improved to 1×10^{-8} Torr soon. Installing the ionized source/gun will further enhance the evenness of the coated surface and increase the reflectivity, especially for wavelengths down to 180 nm. The fully upgraded setup will ensure delivering the optical component with the required reflectivity.

Due to the large quantities of mirrors and focusing cones, it is critical to emphasize that the “semi-industrial” effort for coating these substrates requires significant investment. These investments include refurbishing obsolete equipment, building up an inventory of critical components, cleaning procedures, storage facilities, and a quality assurance station.

4.2 ECal and SPD

In this section we report on the design update of the ECal as well as two beam tests that were carried out at Fermilab Test Beam Facility (FTBF) in January 2021 and JLab’s Hall C in 2022-2023, respectively.

4.2.1 Design updates

Two changes are being planned for the ECal and SPD compared with the 2019 pre-CDR design. First, all of pre-shower and shower modules, as well as forward-angle SPD (FASPD), required the connection of WLS fibers, embedded in individual modules, to clear fibers for readout by PMTs in a low-field region outside the solenoidal field. The requirements on the clear fiber include a long decay length and sufficient radiation hardness. The 2019 design used polystyrene-based clear fibers with PMMA cladding, which are readily available from known vendors such as Saint Gobain (now known as Luxim). Our pre-R&D testing of a variety of clear fibers showed that PMMA-type clear fibers have a longer decay length ($\approx 10\text{ m}$ vs. the 4 m of Luxim fibers), while providing sufficient radiation hardness. These options reduce

the cost significantly. Therefore, we will use PMMA-based clear fibers for all preshower, shower, and FASPD readout moving forward.

The second change is on the large-angle SPD (LASPD) readout, due to the availability of the photosensors on the market. The timing resolution needed from the LASPD requires high photoelectron statistics, which means that the readout photosensor needs to be placed directly on the LASPD, in a high field (1.5 T) region. The 2019 design included fine-mesh PMTs (FMPMTs) which are field-resistant and radiation hard. However, FMPMTs have been discontinued by the vendor. We are currently planning to use microchannel plate (MCP)-based photosensors. These MCP-PMTs are available both as established products from known vendors e.g. Hamamatsu and as new products from developing vendors e.g. Incom. We plan to procure some MCP-PMTs for testing.

4.2.2 ECal test at FTBF 2021

The first beam test of SoLID ECal was carried out in the MT6.2B region of the FTBF from Jan. 13 to 27, 2021. The main goal of the FTBF test was to determine the energy and position resolution of the ECal. The test setup consisted of triggering scintillators, a 1.2-cm thick lead layer, and 3 pre-shower and 3 shashlyk shower modules. Beam energies of 1, 2, 4, 6, 8, 10, 12 and 16 GeV were used with accumulated electron trigger no less than 1M per energy setting. The beam was the secondary beam of FTBF and consists a mixture of electrons, pions and kaons, thus sufficient statistics were also collected for pion events (MIPs). The Multi-Wire Proportional Chambers (MWPCs) of FTBF were used to provide beam position information, and the Cherenkov detector of FTBF provided particle identification. To calibrate the ECal modules, the beam was centered at each module and the calibration constant was determined by aligning the MIP peak to the same position for all 3 modules. The process is repeated for the three pre-shower modules.

The particle position resolution was obtained by comparing the energy cluster center of the three modules and the position information from FTBF's MWPC. The position resolutions of ECal are found to be at 0.6-0.7 cm level, see the left panel of Fig. 4. Similarly, our results on the ECal energy resolution using the FTBF data are shown in the right panel of Fig. 4. The two-parameter fit to the energy resolution gave $\frac{\delta E}{E} = 4.6\% \oplus \frac{10.4\%}{\sqrt{E(\text{GeV})}}$. We estimate that the true energy resolution of the ECal to be slightly better because of two factors related to the FTBF beam quality that are not being corrected: first is the (2-3)% intrinsic energy spread of the beam energy; second is the pileup effects caused by the very high instantaneous particle intensity. The FTBF beam test analysis is now complete, and we conclude that both the position and the energy resolution of the ECal satisfy the SoLID physics and design requirements.

4.2.3 Detector test in JLab Hall C 2022-2023

In summer 2022 through March 2023, a nearly full set of SoLID's detectors – including large-angle scintillator-pad detector (LASPD), GEM, light-gas Cherenkov counter, and electromagnetic calorimeter (ECal) – were tested in Hall C at JLab with the goal being a test of ECal and SPD as well as a combined performance of all detectors under a high rate, high background and high radiation environment.

High quality data were obtained with the detectors placed in an open area at 18° from the beamline, supplemental data were also taken at 7° and 82°. The electron beam energy was 10.6 GeV and the beam current ranged from 5 to 70 μA , while the target included carbon foils, 10-cm long liquid deuterium and hydrogen. While the luminosity of the 2022/23 beam test was below that expected in the SoLID PVDIS experiment, the low energy background incident on the detectors was comparable or above. The beam test luminosity and background were both higher than the SIDIS and J/ψ expected running conditions.

The data collected in this beam test helped benchmarking the simulation on which the SoLID physics program was designed. The data rate agreed with GEANT4-based simulations to within 15% at both 7°

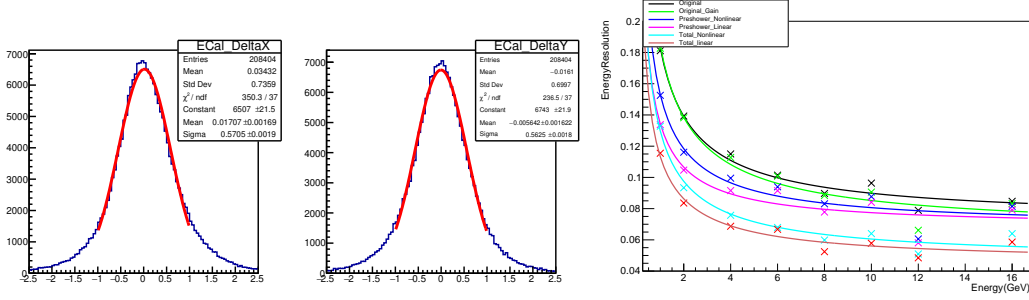


Figure 4: SoLID ECal test results using FTBF data. Left: Position resolution, showing under 1 cm for both X and Y directions. Right: Energy resolution dE/E vs beam energy E (crosses), fitted with $dE/E = \sqrt{p_0^2 + p_1^2/E}$ (curves). A variety of calibration and correction was applied that include: gain matching of the 3 blocks, pre-shower vs. shower matching (both non-linear and linear methods), and finally position dependence caused by the inactive material gap between modules. The corrections reduced the fitted parameter from $\delta E/E = 7.2\% \oplus 16.8\%/\sqrt{E(\text{GeV})}$ (black curve) to $\delta E/E = 4.6\% \oplus 10.4\%/\sqrt{E(\text{GeV})}$ (red curve).

and 18° , although detailed tuning in the ECAL may be needed for the MIP rate. All of the scintillators and preshower detectors performed well and were stable. On the other hand, the readout of the shower modules exhibited unexpected behavior due to the use of passive dividers that caused HV redistribution among dynodes at high rates. This can be mitigated with the use of active HV dividers so long as all components are proven to be radiation-hard.

The ECal plays a critical role in the SoLID physics program. The particle identification performance of the ECal extracted from the beam test data was found to be in agreement with the simulation and meets the requirements of the SoLID physics program. Furthermore, the beam test provided valuable data for AI/ML-based GEM tracking and PID algorithm, for which work is still ongoing.

4.3 GEM

The main challenge for the SoLID GEM detectors is operating large-area GEM detectors in a high-rate, high-background environment. Given this, highly valuable experience for SoLID GEM development is being gathered from operating large-area GEM trackers in the SBS project experiments under high rate conditions approaching the rates expected in SoLID.

So far, in SBS GMn, GEn-II, and nTPE experiments, the GEM trackers have been used for over 14 months in a beam under luminosity conditions unprecedented for large-area GEM detectors. During the GEn-II experiment, data was taken with up to $45 \mu\text{A}$ beam current on a 60 cm polarized ^3He target. This is about a factor of 5 higher than planned for SoLID polarized ^3He target SIDIS experiments. During the GMn experiment, the Bigbite (BB) GEM tracker was routinely operated at a luminosity of approximately 1×10^{38} electron-nucleon $\text{cm}^{-2}\text{s}^{-1}$. Furthermore, high current test runs were taken with the 15 cm liquid deuterium target up to a luminosity of 3×10^{38} electron-nucleon $\text{cm}^{-2}\text{s}^{-1}$. In the upcoming GEp-V experiment, the luminosity is expected to be close to 5×10^{38} electron-nucleon $\text{cm}^{-2}\text{s}^{-1}$. It should be noted that given the baffle structure in the PVDIS configuration, the total exposure of the GEM detectors and the simulated average GEM occupancy levels for the PVDIS case is less than the occupancy levels already achieved in the SBS experiments.

Two GEM trackers have been used in the SBS project so far: (i) BB GEM tracker for electron detection with four layers of $150 \times 40 \text{ cm}^2$ GEM detectors and one layer of $60 \times 200 \text{ cm}^2$ total area made of four $60 \times 50 \text{ cm}^2$ GEM modules; (ii) SBS GEM tracker for proton detection made of 6 layers

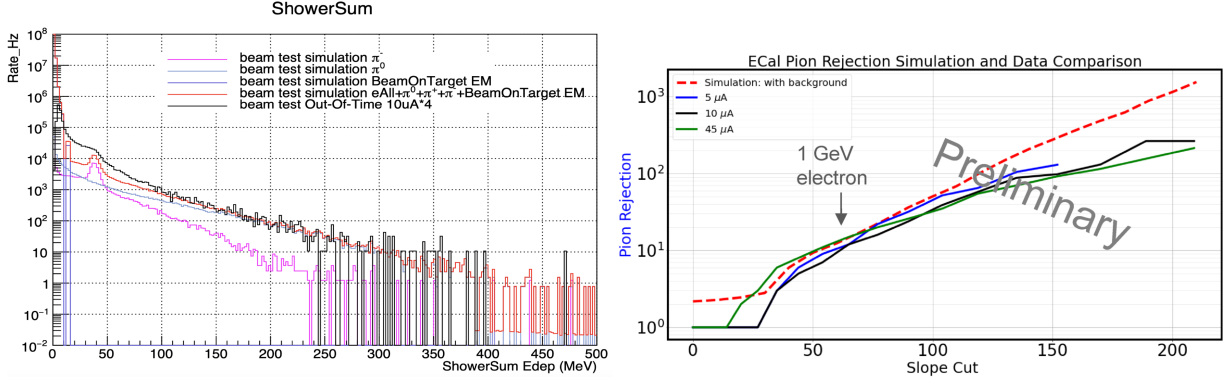


Figure 5: Results from the 2022-2023 Hall C detector beam test. *Left:* Comparison of the total energy deposit in the three Shower modules between data (black) and sum of all simulations (red), showing excellent agreement in the region above the MIP. At the MIP, the simulation is lower than data by about a factor 2, which can be attributed to either low statistics in the simulation of the beam-on-target electromagnetic (EM) background (blue), or that fine-tuning is needed for the charged pion background (magenta); *Right:* Pion rejection factor for selected “Slope Cut” (a cut on the pre-shower and shower total energy deposit) as extracted from pion sample data of varying beam currents (blue, black and green curves), compared with that from the simulation (red dashed curve). The arrow shows the energy deposit that corresponds to electrons of 1 GeV/c momentum. Further improvement is expected once these pion sample events are cleaned up using truth information in the simulation.

of $60 \times 200 \text{ cm}^2$ total area consisting of $60 \times 50 \text{ cm}^2$ GEM modules. The active areas of the $150 \times 40 \text{ cm}^2$ modules used in SBS exceed the active areas of the largest GEM detectors proposed for SoLID.

So far, in more than 14 months of high luminosity in-beam operation, the SBS GEM detectors have functioned very well, as indicated by the following:

- Stable operation of the GEMs: high voltage trips were limited to a level that was not disruptive to the running of the experiments.
- Robust under harsh conditions; so far, only 1 out of the 32 detectors in the beam had to be swapped out due to a suspected short in one of 30 sectors in that detector.
- No radiation damage or aging effects observed; detector performance has remained steady.
- Noise levels sufficiently low and detector gains under stable high voltage conditions sufficiently high to achieve a signal-to-noise ratio of 10 or more under beam conditions.
- Very good spatial resolution of approximately $70 \mu\text{m}$ for tracks incident perpendicular to the detector plane.

The main lesson learned in the SBS GEM operation is that the current drain into GEM detectors operating under high luminosity conditions is too high for the low-cost resistive voltage divider-based GEM high voltage supply scheme to handle. Under high-rate conditions, the currents drawn into GEM foils significantly modify the current flow in the resistive voltage divider chain, decreasing the voltages supplied to the GEM foils. This lowers the avalanche multiplication levels in the GEM holes, lowering the detector gain and efficiency. Due to this effect, the efficiency of SBS GEMs dropped from over 90% in low current operation to around 70% in high current operation. This issue could be fixed using high-voltage power supplies providing the requisite high voltage to each GEM electrode. Such a power

supply was tested during the GEn-II experiment with the $150 \times 40 \text{ cm}^2$ GEM detector exposed to the highest rate in the GEM tracker and was shown to solve the issue. Based on this, all GEM detectors are equipped with individual voltage power supplies for the remaining SBS experiments. A similar power supply scheme will also be adapted for SoLID GEM detectors.

4.4 Data Acquisition

Generic pre-R&D activities were proposed to test and validate the SoLID DAQ concepts which are also useful for the ongoing experiments at JLab. These activities were funded by DOE and greatly improved data taking performance for the SBS and NPS experiments, among many others.

Tasks that are specific to the gas Cherenkov counters and GEM detectors, and that were already reported in previous sections, are

- GEM VMM3 readout high rate testing to determine the trigger rate capability, its behavior with pile-up, and the readout performance. An evaluation board was procured and showed that the signal to noise ratio was appropriate for the SoLID GEM readout in the 10 bit readout mode. A prototype VMM board was designed and built to test the 6 bit mode.
- Test of the gas Cherenkov readout with analog sums and MAROC chip: The Cherenkov was read out with FADCs reading the simple sum of the MAPMTs. This scheme proved to be adequate.

Two additional tasks for the DAQ are:

- FADC developments for fast readout and triggering: Fast readout of the FADCs through the VXS backplane was implemented allowing reading out full waveforms without significant dead-time. The calorimeter and Cherenkov triggers were implemented and tested during the Cherenkov counter test run.
- Time of flight using the NALU sampling chip: An ASOC test system was acquired and tested on the bench, and resolution is sufficient for the SPD readout.

As mentioned above, pre-R&D activities on the DAQ greatly improved data taking performance for the ongoing experiments: The FADC readout was upgraded to use the VXS backplane, increasing the bandwidth by about a factor of 16. This scheme was deployed for SuperBigBite calorimeter readout and is fully tested allowing readout of all channels of hadronic calorimeter and BigBite Shower detector with full waveform, without incurring any significant dead time as shown in Fig.6. The calorimeter trigger was implemented and used for the Cherenkov test run in Hall C (see Section 4.1), in the currently running NPS experiment with a slightly different geometry, and will be used for the upcoming SBS GEp-V experiment.

There are many other developments related to FADC readout and data processing from ongoing experiments that are relevant for SoLID. One example is the treatment of signal pileup, such as those seen in the NPS calorimeter. By fitting individual pulses as shown, the energy resolution of the NPS calorimeter was greatly improved; see Fig. 7. We consider most of the development of the FADC readout and trigger to be no risk as it will be fully tested by the time SoLID installation starts.

On the GEM readout part, the current baseline design is to use VMM chip based system. The VMM chip is radiation hard and has built-in ADC's and TDC's which allows zero suppression to be carried out on the chip. It also features several high speed links allowing operation at high trigger and data rates. The chip was designed to be able to handle up to 4 MHz of rate per channel. Evaluation VMM boards were procured, and their performance reading out a GEM chamber was studied with a radioactive source and cosmic rays. The signal-to-noise ratio is adequate in the 10-bit mode with a 250-ns integration time, which will be sufficient for the SIDIS experiment up to 200 KHz.

A fast readout (shorter dead-time) option with 6-bit was also studied. A VMM prototype board was designed and produced, as shown in Fig.9. It was used to evaluate the 6-bit readout with a 25-ns integration time, which could reduce the deadtime by a factor of 2 for the strips with the highest rate for the PVDIS experiment. The deadtime was checked to be of the order of 90 ns with a 25 ns shaping time. The front-end was checked to ensure it is not saturated by high rate of incoming signal as shown in Fig. 10.

From preliminary studies of the VMM, the chip is well characterized. Expected efficiencies for 50 ns shaping time, are shown in Fig.11, even with 50 ns shaping time the tracking efficiency is acceptable for J/Psi.

Depending on the timing, we are keeping options open to integrate possible future higher performance chips for a similar cost as the VMM. The EIC GEM and Micromegas readout chip is a good potential candidate. More testing is on-going and we planned to test the prototypes in the beam for rate capability and radiation hardness.

SoLID DAQ is fairly low risk as it relies on already proven technologies and will be thoroughly tested during SBS and Moller experiments. The budget was updated reflecting cost increase from VME CPUs, crates and VTPs due to cost of components and inflation.

5 Simulation and Software

As a complex spectrometer with many components, SoLID simulation is crucial for optimizing the design of all subsystems to meet the physics requirements. We continue to develop the simulation to add more realistic details and improve the design. For instance, the magnet endcap is extended 45 cm further downstream to better house the detector subsystems. The magnet field calculation was improved to match the latest design with spare irons from CLEO. The GEM digitization and tracking were adjusted to the new generation of readout electronics.

Detailed simulation studies were carried out for the beam tests of 2018 and 2020 for the Cherenkov detectors and in 2021 and 2022 for the EM Calorimeter. The data taken from the tests were then used to benchmark and tune the simulations. SoLID detector prototypes were implemented in the SoLID Geant4 simulation. The targets, target scattering chamber, and beam line were added according to their technical designs. The high energy electrons and hadrons are produced with event generators and the low energy background particle are generated through beam electrons interacting with the target materials by Geant4

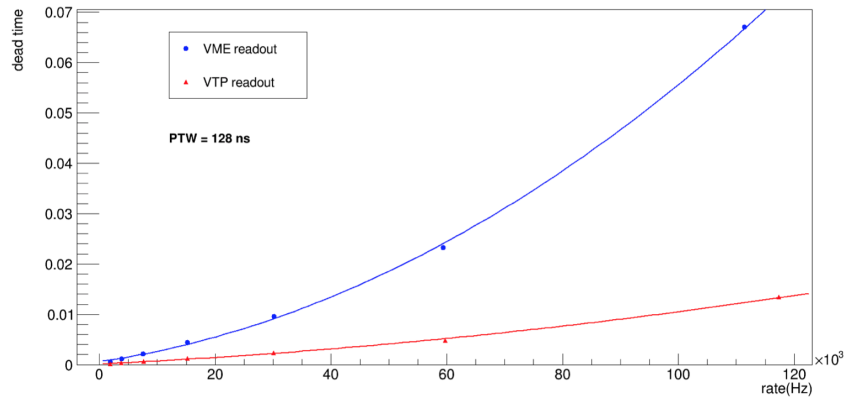


Figure 6: Dead time for FADC readout for 128 samples and 16 channels as a function of trigger rate.

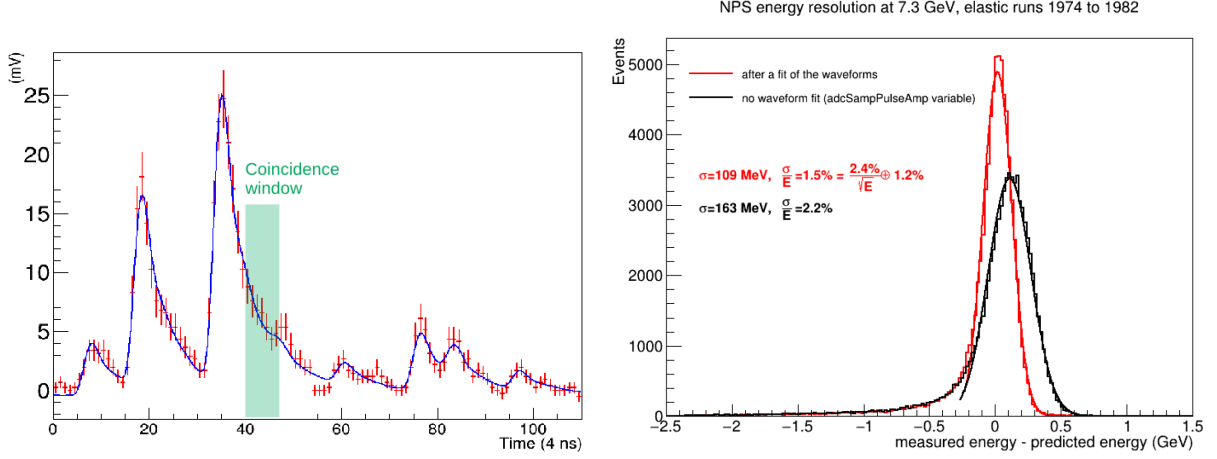


Figure 7: *Left*: Example of signal pile-up in NPS PbWO₄ calorimeters. *Right*: NPS calorimeter resolution with (red) and without (black) waveform fitting. The resolution improved from 2.2% to 1.5%.

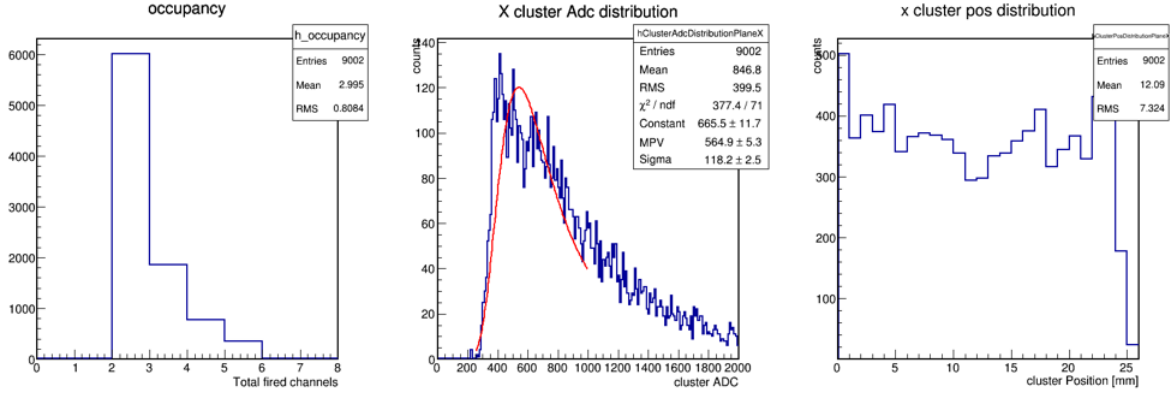


Figure 8: Cosmics spectrum of 10cmX10cm takem with VMM evaluation board

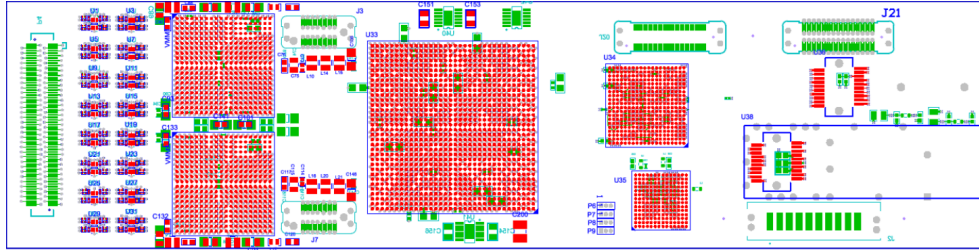


Figure 9: Schematics of VMM prototype board

directly. Simulation of the beam tests is considered a milestone of the SoLID simulation development. The results are used not only to interpret the test data but also to project the SoLID performance under the expected running conditions.

Several event generators were developed and improved for various physics studies. The inclusive electron generator “evgen_inclusive_e” [19], which includes Quasi-Elastic scattering, resonance scattering, and Deep Inelastic Scattering (DIS), is based on fit to existing data and agrees with the inclusive cross sections of the MARATHON experiment [20] within 10 – 30%. The inclusive hadron events are

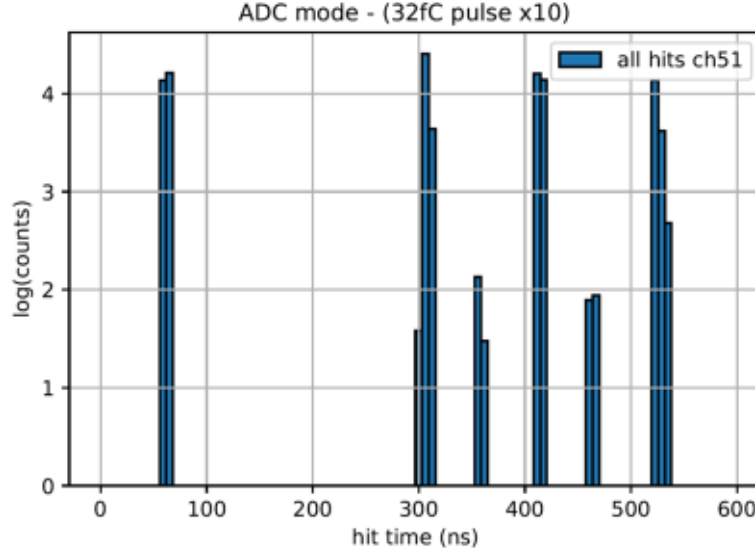


Figure 10: Hits as a function of time with 20 MHz pulses at input. As expected, we miss hits after the dead time from the first hit.

generated with the “evgen_bggen” event generator [21] which is based on fit to data and PYTHIA. Single π^- cross section calculated from the “evgen_bggen” generator agrees with the MARATHON data [22] at 30% level. Furthermore, the cross-section of π^0 , the main background source of high energy photons, is consistent with that extracted from the DVCS experiment [23] within 20 – 30%.

The SoLID simulation and analysis has been relying on the Geant4 based GEMC [24] simulation framework and ROOT based simple script tools. We are testing a more comprehensive software stack which is similar to what the ePIC collaboration uses for the electron-ion collider (EIC) experiments. It includes DD4HEP for the geometry description, JANA2 for event processing and reconstruction, and EDM4HEP for the data model. These software packages are being actively developed and maintained by both the high-energy physics and the nuclear physics communities. That software stack is expected to utilize high-performance computing resources for the simulation and analysis of the next-generation of medium energy nuclear physics experiments. SoLID experiments expect the need for large-scale simulations and data analyses at the luminosity frontier, and this software stack is suitable for these tasks. In addition, the sharing of the new software stack would be mutually beneficial for both the SoLID and ePIC collaborations. On one hand, The two collaborations both contribute to the maintenance and development, reducing the workforce needed by each collaboration for the software work. On the other hand, the implementation of extremely high-rate simulation for the SoLID overall physics program would also test the robustness of the software and probably help improve its performance. The transition testing has been initiated. A crude SoLID geometry has already been implemented in the DD4Hep. Digitization and reconstruction chains for the EM calorimeters and Cherenkov detectors have also been created and will be under a thorough comparison with the original simulations and the beam test data.

6 Cost Estimation Update and Optional Cost Sharing Plan

Cost estimations for SoLID were carried out a few times before the DOE Science Review in 2021. The first cost estimation was performed for the 2014 version of the pCDR submitted to the JLab management in preparation for the JLab Director’s Review in 2015. The cost estimation was updated in 2017. For

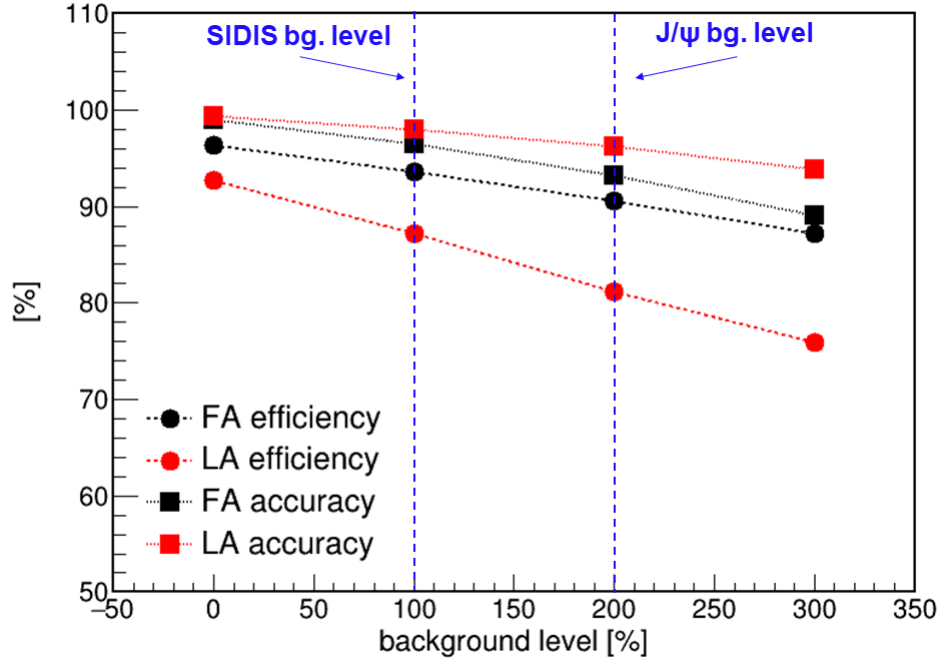


Figure 11: Tracking efficiency for 50 ns shaping time for different level of background. This show that this settings give adequation tracking efficiency for SIDIS and J/Psi experiments

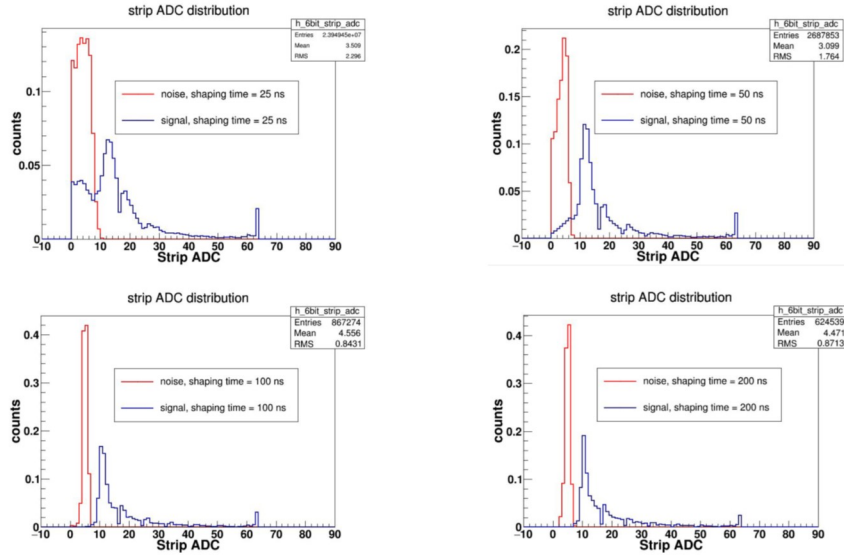


Figure 12: Signal and pedestal for different integration time for the 6 bit mode using Sr90 source, while the MIP amplitude does not significantly change, pedestal width increases as shaping timing decreases. The 50 ns shaping time seems is optimal right now. The 25 ns shaping could be used if signal to noise is improved which is being investigated now.

the 2019 version of the pCDR, the cost estimation was updated and this pCDR was submitted by JLab to DOE as part of the MIE. It was rechecked before the 2021 DOE Science Review of SoLID. After the submission of the SoLID MIE in early 2020, there were pre-R&D activities performed on all subsystems,

including the DOE-funded beam tests of detectors and DAQ system, which helped validate the pre-conceptual design and reduce the technical, cost, and schedule risks. To capture all the updates we recently performed one more round of cost estimation.

Procurement costs were updated with new quotations from the vendors wherever they were provided. The labor cost used the latest (2023) labor and overhead rates from JLab and user groups. Contingencies were included in the cost estimation. Escalations were also included with an assumed spending profile.

With the high priority recommendation of SoLID in the Long-Range-Plan and the crucial role SoLID would play in realizing the full physics potential of JLab, and in consultation with DOE, JLab has been looking into an optional plan by reallocating lab's resource to help share part of the cost of SoLID. A portion of the DAQ cost was moved to be dependency by expanding JLab Physics Division generic electronics pool using capital accounts to purchase pipeline DAQ instrumentation (such as FADCs). In the recent discussion, an option is under consideration in which JLab would use part of the Capital Funds to share part of the cost for GEM and Light Gas Cherenkov detectors. JLab would also use operation funds to support extending the CLEO II solenoid magnet testing to full current.

Bibliography

- [1] “SoLID PreCDR 2019.”
<https://solid.jlab.org/DocDB/0002/000282/001/solid-precdr-2019Nov.pdf>.
- [2] J.-P. Chen, H. Gao (contact), J.-C. Peng, X. Qian et al., “Target Single Spin Asymmetry in Semi-Inclusive Deep-Inelastic ($e, e'\pi^\pm$) Reaction on a Transversely Polarized ^3He Target at 11 GeV.” Jefferson Lab Experiment E12-10-006, 2010 with 2022 update.
- [3] J.-P. Chen (contact), J. Huang, C. Peng, W.-B. Yan et al., “Asymmetries in Semi-Inclusive Deep-Inelastic ($e, e'\pi^\pm$) Reactions on a Longitudinally Polarized ^3He Target at 8.8 and 11 GeV.” Jefferson Lab Experiment E12-11-007, 2011 with 2022 update.
- [4] J.-P. Chen, H. Gao (contact), V. Khachatryan, X. Li, Z.-E. Meziani et al., “Target Single Spin Asymmetry in Semi-Inclusive Deep-Inelastic ($e, e'\pi^\pm$) Reaction on a Transversely Polarized Proton Target.” Jefferson Lab Experiment E12-11-108, 2011 with 2022 update.
- [5] S. Joosten, Z.-E. Meziani (contact), X. Qian, N. Sparveris, Z. Zhao et al., “Near Threshold Electroproduction of J/Ψ at 11 GeV.” Jefferson Lab Experiment E12-12-006, 2012 with 2022 update.
- [6] P. A. Souder (contact), P. E. Reimer, X. Zheng et al., “Precision Measurement of Parity-violation in Deep Inelastic Scattering Over a Broad Kinematic Range.” Jefferson Lab Experiment E12-10-007, 2010 with 2022 update.
- [7] G. M. Huber (contact), Z. Ahmed, Z. Ye et al., “Measurement of Deep Exclusive π^- Production using a Transversely polarized ^3He Target and the SoLID Spectrometer.” Jefferson Lab Run Group Experiment E12-10-006B, 2017.
- [8] M. Boer, P. Nadel-Turonski, J. Zhang, Z. Zhao (contact) et al., “Timelike Compton Scattering on the proton in e^+e^- pair production with SoLID at 11 GeV.” Jefferson Lab Run Group Experiment E12-12-006A, 2015.
- [9] W. R. Armstrong, S. J. Joosten, C. Peng, Y. Tian (contact), W. Xiong, Z. Zhao et al., “A Precision Measurement of Inclusive g_2^n and d_2^n with SoLID on a Polarized ^3He Target at 8.8 and 11 GeV.” Jefferson Lab Rungroup Experiment E12-11-007A/E12-10-006E, 2020.
- [10] J. Arrington (contact), R. Beminiwattha, D. Gaskell, J. Mammei, P. Reimer et al., “First Measurement of the Flavor Dependence of Nuclear PDF Modification Using Parity-Violating Deep Inelastic Scattering.” Jefferson Lab Proposal PR12-22-002, 2022.
- [11] M. Nycz (contact), W. Henry, Y. Tian, W. Xiong, X. Zheng et al., “Measurement of the Beam Normal Single Spin Asymmetry in Deep Inelastic Scattering using the SoLID Spectrometer.” Jefferson Lab Experiment E12-22-004, 2022.
- [12] A. Camsonne (contact), M. Boer, E. Voutier, Z. Zhao et al., “Measurement of Double Deeply Virtual Compton Scattering in the di-muon channel with the SoLID spectrometer.” Jefferson Lab Letter-of-Intent LOI12-23-012, 2023.
- [13] U.S. Nuclear Science Advisory Committee, “A New Era of Discovery, the 2023 Long Range Plan for Nuclear Science.” <https://nuclearsciencefuture.org/>, 2023.

- [14] A. Accardi et al., *An experimental program with high duty-cycle polarized and unpolarized positron beams at Jefferson Lab*, *Eur. Phys. J. A* **57** (2021) 261, [2007.15081].
- [15] N. Alamanos, M. Battaglieri, D. Higinbotham, S. Niccolai, A. Schmidt and E. Voutier, *Topical issue on an experimental program with positron beams at Jefferson Lab*, *Eur. Phys. J. A* **58** (2022) 45.
- [16] A. Accardi et al., *Strong Interaction Physics at the Luminosity Frontier with 22 GeV Electrons at Jefferson Lab*, 2306.09360.
- [17] C. Peng et al., *Performance of photosensors in a high-rate environment for gas Cherenkov detectors*, *JINST* **17** (2022) P08022, [2011.11769].
- [18] J. Xie et al., *Performance of a coarsely pixelated LAPPD photosensor for the SoLID gas Cherenkov detectors*, 2402.00947.
- [19] evgen_inclusive_e, https://github.com/jeffersonlab/evgen_inclusive_e, .
- [20] J. Bane, *The EMC Effect in A=3 Nuclei.*, Ph.D. Dissertation, University of Tennessee, 2019.
- [21] evgen_bggen, https://github.com/jeffersonlab/evgen_bggen, .
- [22] Z. Ye, *Private communications*, .
- [23] Y. Tian, *Ph.D. thesis*, .
- [24] GEMC, <https://gemc.jlab.org>, .

A PAC 50 Report on SoLID-related Proposals

Introduction

The Jefferson Lab Program Advisory Committee held its 50th meeting from July 11th through July 24th, 2022. The membership of the committee is given on page 34. In response to the charge (page 35) from the former JLab Deputy Director, Dr. Robert McKeown, the committee reviewed 6 new proposals, 3 conditional proposals, 5 Jeopardy proposals, 1 run group addition and 2 letters of intent.

PAC 50 SUMMARY OF RECOMMENDATIONS								
Number	Contact Person	Title	Hall	Days Req'd	Days Awarded	Scientific Rating	PAC Decision	Topic
C12-21-004	L. Weinstein	Semi-Inclusive Deep Inelastic Scattering Measurement of A=3 Nuclei with CLAS12 in Hall B	B	58			C2	1
C12-21-003	A. Gasparian	A Direct Detection Search for Hidden Sector New Particles in the 3-60 MeV Mass Range	B	60	60	A	Approved	Other
C12-18-005	M. Boer	Timelike Compton Scattering off a Transversely Polarized Proton	C	50			Deferred	4
PR12-22-001	N. Sparveris	Measurement of the N to Delta Transition Form Factors at low four momentum transfers	C	11	11	A-	Approved	2
PR12-22-002	J. Arrington	First Measurement of the Flavor Dependence of Nuclear PDF Modification Using Parity-Violating Deep Inelastic Scattering	A	83			C2	5
PR12-22-003	I. Larin	Precision Measurement of the Neutral Pion Transition Form Factor	B	67	67	A-	Approved	6
PR12-22-004	M. Nycz	Measurement of the Beam Normal Single Spin Asymmetry in Deep Inelastic Scattering using the SOLID Detector	A	38	38	A-	Approved	Other
PR12-22-005	B. Wojtsekhowski	A Search for a Nonzero Strange Form Factor of the Proton at 2.5 (GeV/c) ²	C	35			Deferred	2
PR12-22-006	C. Munoz Camacho	Deeply Virtual Compton Scattering off the neutron with the Neutral Particle Spectrometer in Hall C	C	44	44	A	Approved	4

PAC 50 SUMMARY OF JEOPARDY RECOMMENDATIONS						
Number	Contact Person	Title	Hall	Days Requested (Already taken)	Days Awarded	PAC Decision
E12-10-007	P. Souder	Precision Measurement of Parity-Violation in Deep Inelastic Scattering over a Broad Kinematic Range	A	338	169	Remain active
E12-12-006	Z.-E. Meziani	Near-Threshold Electroproduction of J/psi at 11 GeV	A	60	60	Change rating from A- to A
E12-11-007	J.P. Chen	Asymmetries in Semi-Inclusive Deep-Inelastic Electro-Production of Charged Pion on a Longitudinally Polarized He-3 Target at 8.8 and 11 GeV	A	35	35	Remain active
E12-10-006	H. Gao	Target Single Spin Asymmetry in Semi-Inclusive Deep-Inelastic Electro Pion Production on a Transversely Polarized 3He Target at 8.8 and 11 GeV	A	90	90	Remain active
E12-11-108	H. Gao	Target Single Spin Asymmetry in Semi-Inclusive Deep-Inelastic (e, e' π^+) Reaction on a Transversely Polarized Proton Target	A	120	120	Remain active

C1=Conditionally Approved w/Technical Review

C2=Conditionally Approved w/PAC Review